Coulomb gas - RPA & electron renormalization

(1) Jellium model

$$\hat{H} = \sum_{k\sigma} \varepsilon_k \hat{c}^{+}_{k\sigma} \hat{c}_{k\sigma} + \hat{H}_{e\text{-}e} + \hat{V}_{ext}$$

system assumed **fully homogeneous**
(ok for simple metals like Na)

- non-perturbed Hamiltonian: electrons in a single band

  Free-electron dispersion $\varepsilon_k = \frac{\hbar^2 k^2}{2m} - \mu$

- perturbation I: Coulomb interaction among electrons

$$\hat{H}_{e\text{-}e} = \frac{1}{2} \sum_{\substack{k k' q \\ \sigma\sigma'}} V_q \hat{c}^{+}_{k+q\sigma} \hat{c}^{+}_{k'-q\sigma'} \hat{c}_{k'\sigma'} \hat{c}_{k\sigma} \quad \text{with} \quad V_q = \frac{1}{\Omega} \frac{e^2}{\varepsilon_0 q^2}$$

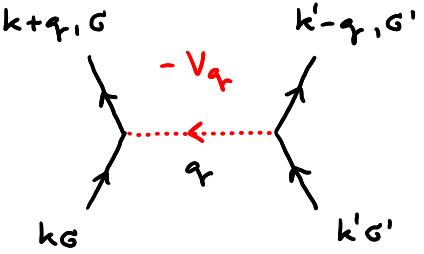

- perturbation II: interaction with the nuclei

$$\hat{V}_{ext} = \sum_{kq} V^{ext}_{k,k+q} \hat{c}^{+}_{k\sigma} \hat{c}_{k+q\sigma} \quad \text{with} \quad V^{ext}_{k,k+q} = -\frac{e^2 n_0}{\varepsilon_0 q^2} \delta_{k,k+q}$$

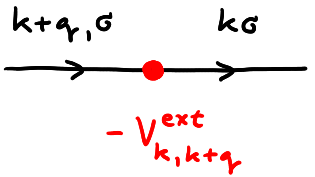

② Selfenergy

- expansion of single-particle propagator (only e-e Coulomb interaction included)

0th and 1st order

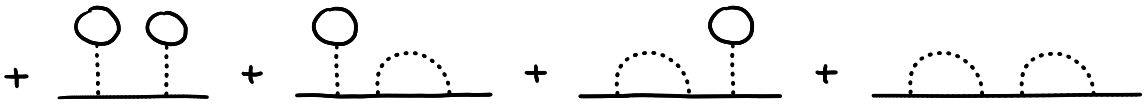

2nd order reducible

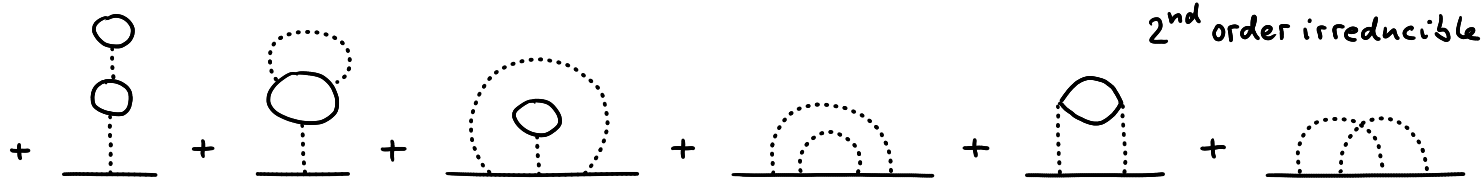

2nd order irreducible

+ higher orders

improper selfenergy :

all possible insertions

proper selfenergy :

only the irreducible insertions

- **Dyson's equation**

(+ spin conservation)

$$-G(k,iE) \qquad -G_0(k,iE) \qquad [-G_0(k,iE)][-\Sigma(k,iE)][-G(k,iE)]$$

$$\rightarrow \quad G = G_0 + G_0 \Sigma G \quad \text{by dividing by } G G_0 \rightarrow \quad G^{-1} = G_0^{-1} - \Sigma$$

electron propagator including selfenergy corrections

$$G(k,iE_n) = \frac{1}{iE_n - \varepsilon_k - \Sigma(k,iE_n)} \qquad (\varepsilon_k \text{ includes } \mu)$$

- **selfenergy expansion**

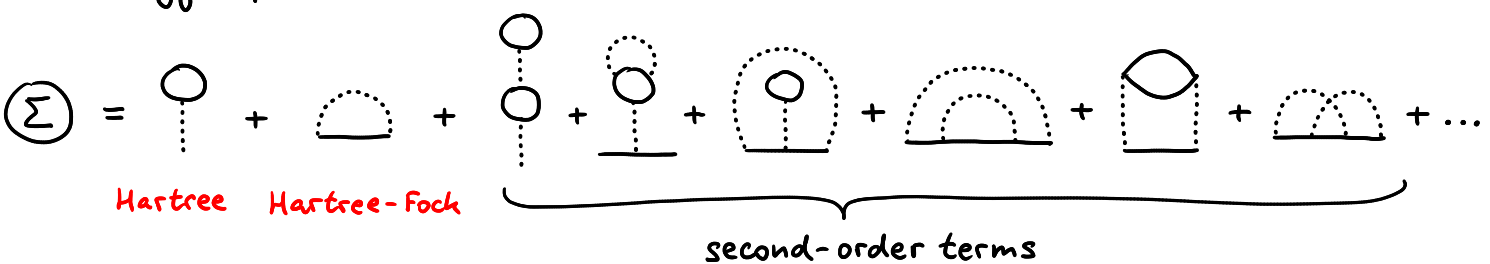

③ Hartree & Hartree-Fock contributions to the selfenergy

- compensation of Hartree selfenergy and interaction with the positive background

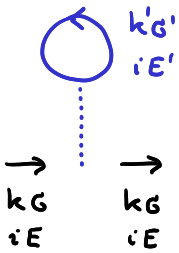

← translated as

$$-\Sigma_H = (-1) \sum_{k'G'} (-V_{q=0}) \frac{1}{\beta} \sum_{iE'} - G_0(k', iE')$$

Fermionic loop — Zero momentum transfer via ..... — single self-closed propagator line

"subtle" detail associated with ⟲..... :

G_0 originates from $\langle T\{ \hat{c}^{+}_{k'G'}(\tau_1^{+}) \hat{c}_{k'G'}(\tau_1) \} \rangle_0 = - G_0(k', 0^-)$

Matsubara representation $G_0(k', \tau) = \frac{1}{\hbar\beta} \sum_{iE_n} G_0(k', iE_n) e^{-iE_n \frac{\tau}{\hbar}}$

use $G_0(k, iE_n) e^{-iE_n 0^-} = \frac{1}{iE_n - \varepsilon_k} e^{-iE_n 0^-}$ as Matsubara coefficients

- to be included in case of a summation linked to a single propagator line

Matsubara sum evaluated to $\frac{1}{\beta}\sum_{iE_n} \frac{e^{-iE_n 0^+}}{iE_n - \varepsilon_k} = n_F(\varepsilon_k)$

electron density $n_0 = \frac{N}{\Omega}$

Hartree selfenergy constant (k, iE independent)

$$\Sigma_H = V_{q=0} \underbrace{\sum_{k'\sigma'} n_F(\varepsilon_{k'})}_{\text{electron count } N} = \frac{e^2 n_0}{\varepsilon_0 q^2}\Big|_{q=0}$$

homogeneous background →

no difference between $\langle c^+c\rangle_0$ and $\langle c^+c\rangle$

compensated by opposite $\hat{V}_{ext}$

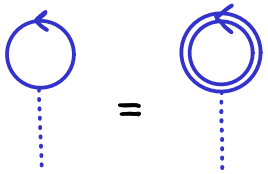

Factor $-\Sigma_H = -\frac{e^2 n_0}{\varepsilon_0 q^2}\Big|_{q=0}$

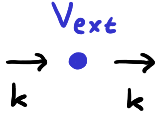

Factor $-V^{ext}_{k,k} = +\frac{e^2 n_0}{\varepsilon_0 q^2}\Big|_{q=0}$

remove all Hartree-like diagrams, i.e. exclude $V_{q=0}$ in the diagrams at all levels

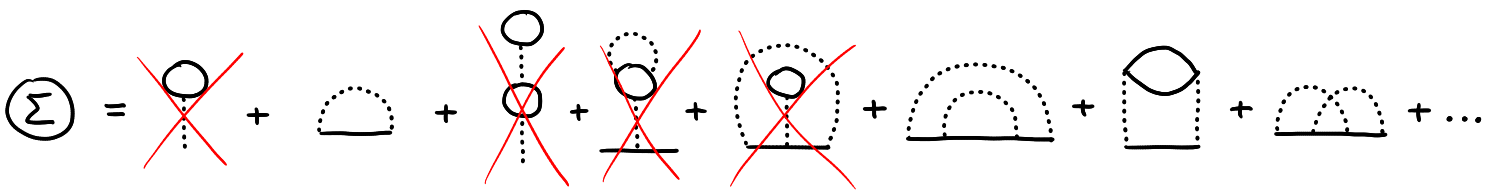

- Hartree - Fock selfenergy

infinitesimal factor as in Hartree term

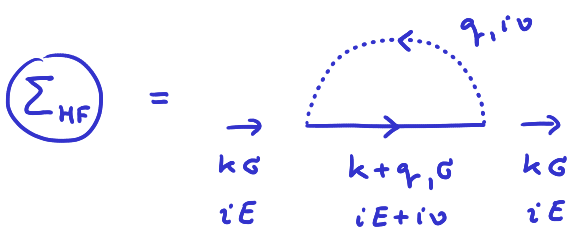

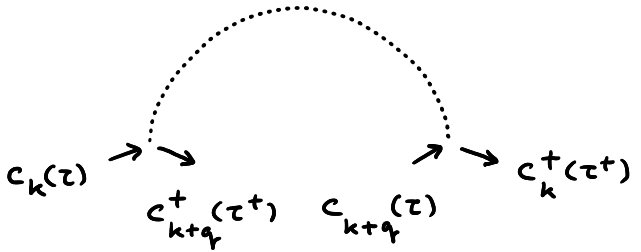

translated

$$-\Sigma_{HF}(k,iE) = \sum_q (-V_q)\, \frac{1}{\beta} \sum_{i\nu} \left[-G_0(k+q, iE+i\nu)\, e^{-(iE+i\nu)0^-} \right]$$

$$\Sigma_{HF}(k) = -\sum_q V_q\, n_F(\varepsilon_{k+q}) = -\sum_{k'} V_{k'-k}\, n_{k'} = -\frac{1}{\Omega} \sum_{k'} \frac{e^2}{\varepsilon_0 |k'-k|^2}\, n_{k'}$$

$$\frac{1}{(2\pi)^3} \int d^3\bar{k}'$$

evaluation at $T=0$

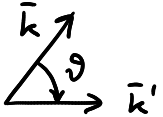

$$\Sigma_{HF}(k) = -\int_{k'<k_F} \frac{d^3\bar{k}'}{(2\pi)^3} \frac{e^2}{\varepsilon_0 (\bar{k}-\bar{k}')^2} = -\frac{1}{(2\pi)^3} \int_0^{k_F} dk'\, k'^2 \int_0^{\pi} d\vartheta \sin\vartheta \int_0^{2\pi} d\varphi\, \frac{e^2}{\varepsilon_0} \frac{1}{k^2+k'^2-2kk'\cos\vartheta}$$

$$= -\frac{e^2}{4\pi^2\varepsilon_0}\int_0^{k_F} dk'\,k'^2 \int_{-1}^{+1} d\xi\,\frac{1}{k^2+k'^2-2kk'\xi} = \ldots = -\frac{e^2}{4\pi^2\varepsilon_0}\,k_F\left(1+\frac{1-x^2}{2x}\ln\left|\frac{1+x}{1-x}\right|\right) \qquad x = k/k_F$$

propagator in H-F approximation

$$G(k,iE) = \frac{1}{iE - \varepsilon_k - \Sigma_{HF}(k)} \longrightarrow \text{new dispersion } \tilde{\varepsilon}_k = \varepsilon_k + \Sigma_{HF}(k)$$

severe problem with the density of states

$$DOS(E) = \sum_k \delta\left[E - \varepsilon_k - \Sigma_{HF}(k)\right] = \iint_{S(E)} \frac{dS}{\left|\nabla_k\left[\varepsilon_k + \Sigma_{HF}(k)\right]\right|} = \frac{4\pi k^2}{\frac{\hbar^2 k}{m} + \frac{\partial \Sigma_{HF}}{\partial k}}\Bigg|_{k(E)}$$

$\frac{\partial \Sigma_{HF}}{\partial k}$ has a log singularity at $k = k_F$ $\longrightarrow$ DOS vanishes at E_F ?

- gets corrected by higher-order terms contributing to Σ

- evaluation of the auxiliary sum using contour integration

complex function $f(z) = \dfrac{n_F(z)}{z-\varepsilon_k} e^{z\Delta}$ with $\Delta \to 0^+$ integrated along closed contour $C_1 + C_2$

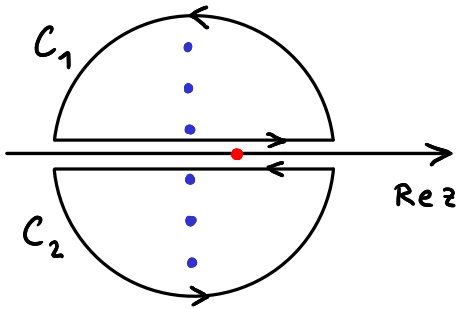

$|z| \to \infty$ semicircles do not contribute

$$\frac{e^{z\Delta}}{e^{\beta z}+1} \approx \begin{cases} e^{-\beta z} \to 0 & \text{Re } z > 0 \\ e^{z\Delta} \to 0 & \text{Re } z < 0 \end{cases}$$

→ integral value determined by the horizontal sections

$$\int_{-\infty}^{\infty} \frac{n_F(E)}{E+i0^+-\varepsilon_k} dE - \int_{-\infty}^{\infty} \frac{n_F(E)}{E-i0^+-\varepsilon_k} dE = \int_{-\infty}^{\infty} n_F(E)\left[-i\pi\delta(E-\varepsilon_k) - i\pi\delta(E-\varepsilon_k)\right] dE = -2\pi i\, n_F(\varepsilon_k)$$

at the same time by residue theorem

$$\oint_{C_1+C_2} \frac{n_F(z)}{z-\varepsilon_k} e^{z0^+} dz = 2\pi i \sum \text{residua at } iE_n = -\frac{1}{\beta} 2\pi i \sum_{iE_n} \frac{e^{iE_n 0^+}}{iE_n - \varepsilon_k}$$

④ RPA - Random-phase approximation

- selection of higher-order terms

relevant second-order contributions to Σ:

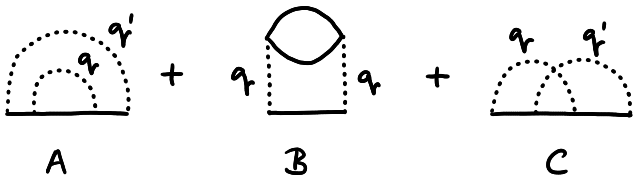

A, C: $\int d^3\bar{q}\, \int d^3\bar{q}'\, V_q V_{q'} \cdots$ safe

B: $\int d^3\bar{q}\, V_q^2 \cdots \sim \int_0^\infty dq\, q^2\, \frac{1}{q^4} \cdots$

→ infrared divergence

→ include only diagrams with the strongest divergence

(maximum number of Coulomb lines with the same q)

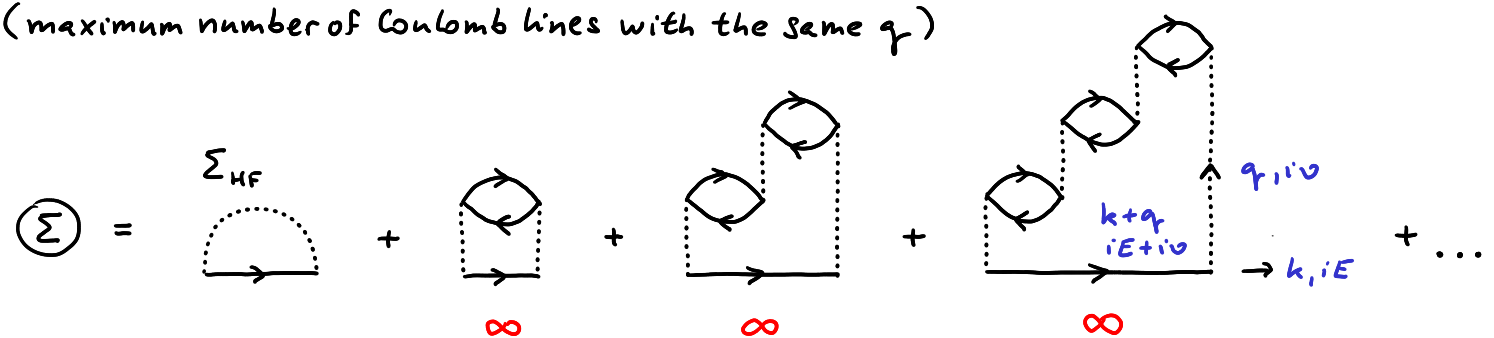

- RPA series

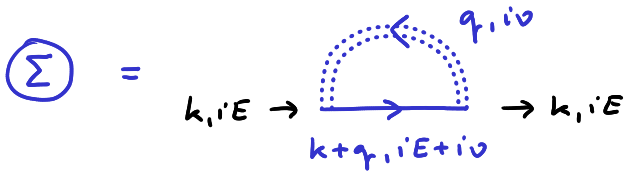

:::::::::: effective interaction:

Coulomb + bubble insertions

geometric series

$-V_{RPA}(q,i\nu)$ $\quad -V_q \quad (-V_q)(\Omega\pi_0)(-V_q) \quad (-V_q)(\Omega\pi_0)(-V_q)(\Omega\pi_0)(-V_q)$

summed up to

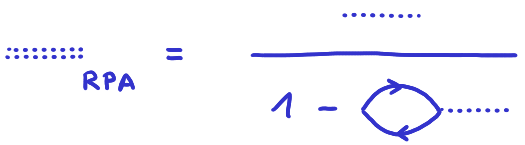

translated $\quad -V_{RPA} = \dfrac{-V_q}{1-(\Omega\pi_0)(-V_q)}$

Final result: $V_{RPA}(q,i\nu) = \dfrac{V_q}{\varepsilon_{RPA}(q,i\nu)}$ with $\varepsilon_{RPA}(q,i\nu) = 1 + \dfrac{e^2}{\varepsilon_0 q^2}\,\Pi_0(q,i\nu)$

- bubble insertion

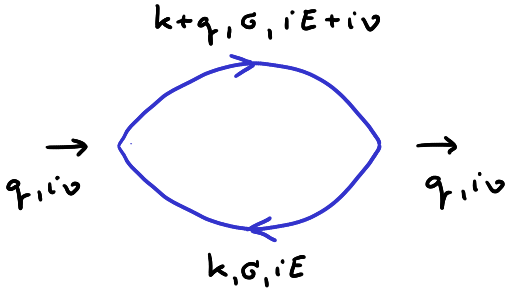

diagram = $\Omega \Pi_0$, Π_0 corresponds to Lindhard function

$$\Pi_0(q, i\nu) = -\frac{1}{\Omega} \sum_{k\sigma} \frac{1}{\beta} \sum_{i\varepsilon} G_0(k+q, i\varepsilon+i\nu)\, G_0(k, i\varepsilon)$$

$$= \frac{2}{\Omega} \sum_{k} \frac{n_F(\varepsilon_k) - n_F(\varepsilon_{k+q})}{\varepsilon_{k+q} - \varepsilon_k - i\nu_m}$$

- connection to diagrammatic expansion of charge susceptibility

interaction with external field

$$\int d^3\vec{r}\, \varphi(\vec{r})\, \rho(\vec{r}) \rightarrow \sum_q \varphi_q \hat{\rho}_{-q}$$

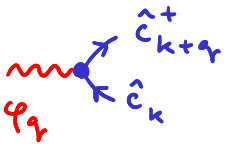

measurement of charge density

$$\hat{\rho}_q = \frac{-e}{\Omega} \sum_{k\sigma} \hat{c}^+_{k\sigma}\, \hat{c}_{k+q\sigma}$$

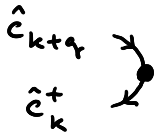

charge susceptibility

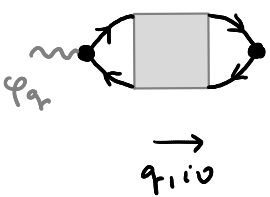

$= \chi_{ch}(q, i\nu)$

(no minus sign here)

- diagrammatic expansion

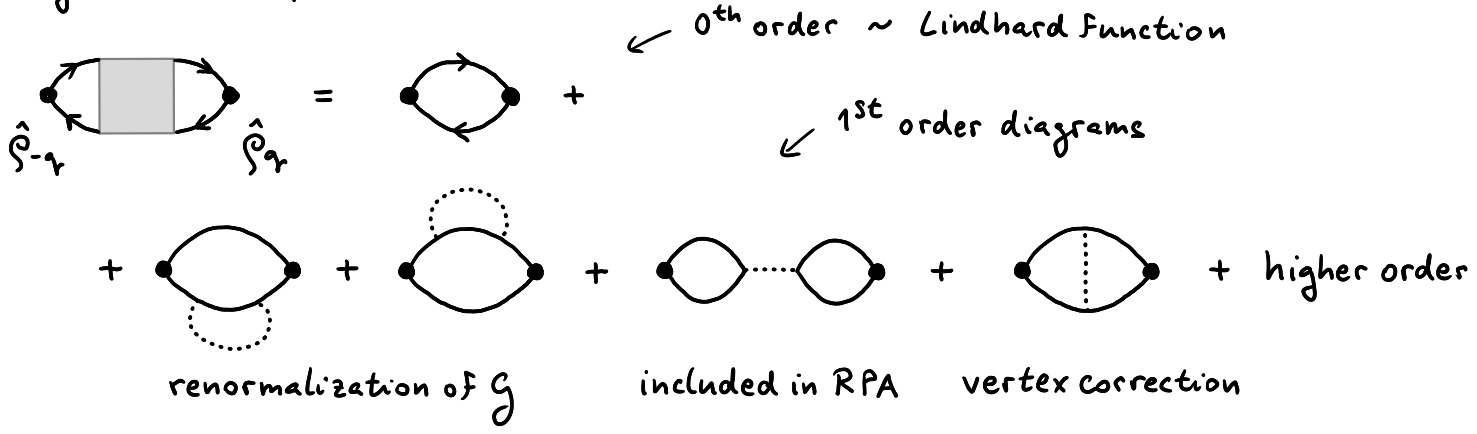

- in RPA approximation

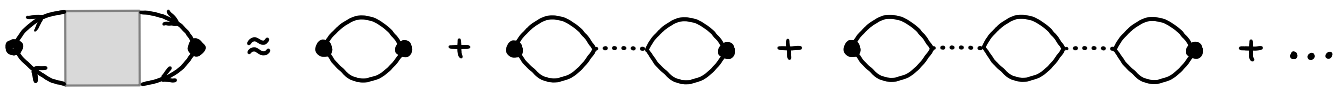

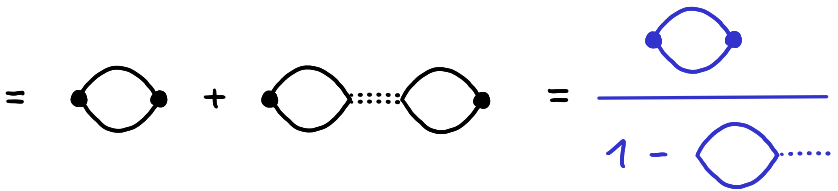

$$\chi_{RPA}(q,i\nu) = \frac{\chi_0(q,i\nu)}{\varepsilon_{RPA}(q,i\nu)}$$

- effective (renormalized) Coulomb interaction

$$\frac{1}{\varepsilon_{RPA}} = \frac{1}{1 - \bigcirc\!\!\!\!\bigcirc\cdots}$$

$$\varepsilon_{RPA}(q,\omega) = 1 + \frac{e^2}{\varepsilon_0 q^2}\,\Pi_0(q,\omega) = 1 + \frac{e^2}{\varepsilon_0 q^2}\,\frac{m k_F}{2\pi^2\hbar^2}\,\tilde{\Pi}_0(q,\omega)$$

dimensionless Lindhard function (Lect. 5)

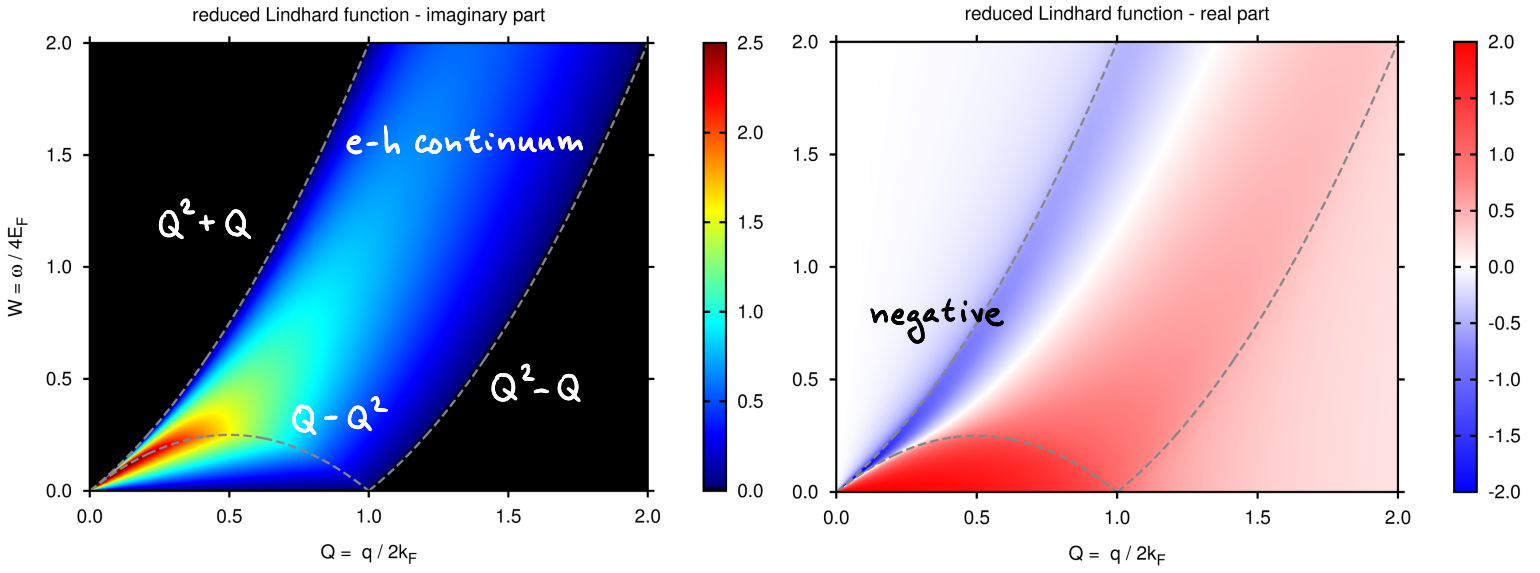

static limit – modified RKKY

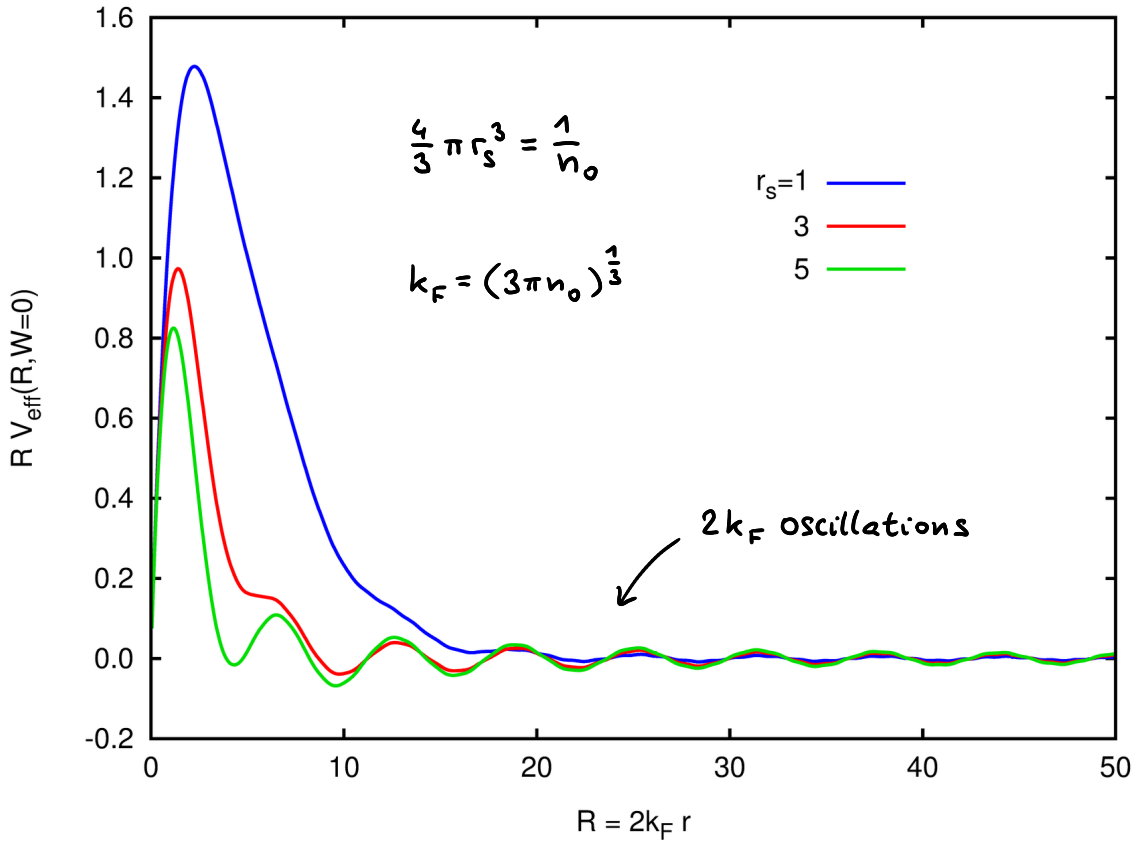

spectral density of the effective interaction

$$B(q,\omega) = -\frac{1}{\pi}\,\mathrm{Im}\left[\frac{1}{\varepsilon_{RPA}(q,\omega)} - 1\right]$$

$$V_{eff}(q,i\nu) = V_q\left[1 + \int_{-\infty}^{\infty} d\omega\, \frac{B(q,\omega)}{i\nu - \omega}\right]$$

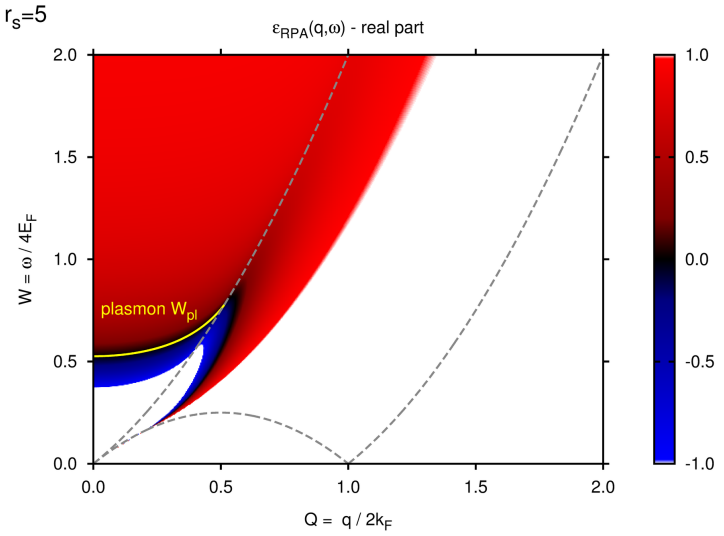

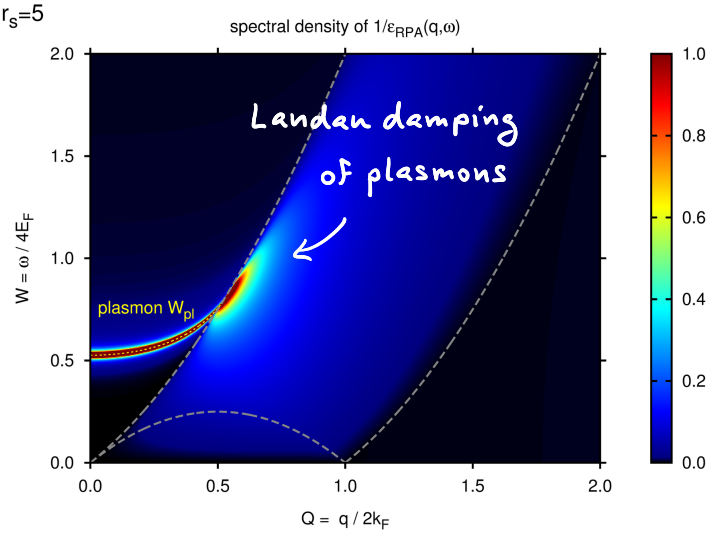

1) particle - hole continuum where $\mathrm{Im}\,\pi_0 \neq 0$

2) plasmon contribution where $\varepsilon_{RPA} = 0$ → collective mode hidden in :::::::

- plasmons – dispersion obtained by solving $\varepsilon_{RPA}(q, \omega_{pl}(q)) = 0$

small-q expansion of $\pi_0(q,\omega)$

$$\mathrm{Re}\,\tilde{\pi}_0(q,\omega) = 1 + \frac{1-(Q-\frac{W}{Q})^2}{4Q}\ln\left|\frac{W-Q^2-Q}{W-Q^2+Q}\right| + \frac{1-(Q+\frac{W}{Q})^2}{4Q}\ln\left|\frac{W+Q^2+Q}{W+Q^2-Q}\right| \approx -\frac{2}{3}\left(\frac{Q}{W}\right)^2 - \frac{2}{5}\left(\frac{Q}{W}\right)^4$$

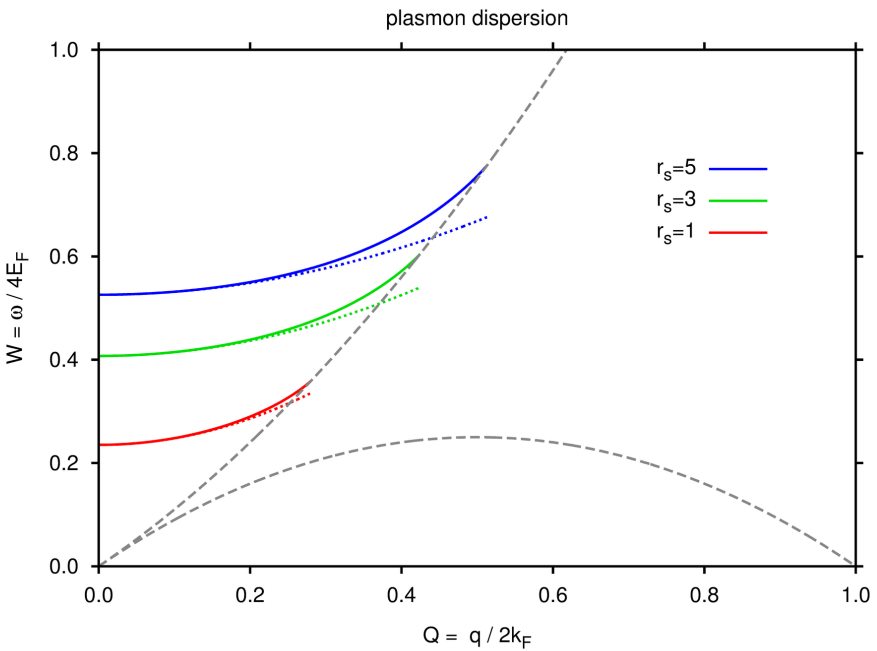

dispersion

$$\omega_{pl}(q) = \omega_{pl}(0) + \alpha\frac{\hbar^2 q^2}{2m}$$

$$\omega_{pl}(0) = \sqrt{\frac{n_0 e^2}{m\varepsilon_0}}$$

$$\alpha_{FE} = \frac{3}{10}\frac{E_F}{\hbar\omega_{pl}} \qquad (FE = \text{free electrons})$$

plasmon approximation for ε:

$$\varepsilon_{RPA} \approx 1 - \frac{\omega_{pl}^2(q)}{\omega^2}$$

5 Plasmons in experiments

PHYSICAL REVIEW VOLUME 175, NUMBER 3 15 NOVEMBER 1968

- plasmon energies via EELS

electron energy loss spectroscopy

Characteristic Energy Losses of 8-keV Electrons in Liquid Al, Bi, In, Ga, Hg, and Au*

C. J. Powell
National Bureau of Standards, Washington, District of Columbia 20234
(Received 14 June 1968)

Characteristic loss spectra have been obtained in a reflection scattering geometry for liquid Al, Bi, In, Ga, Hg, and Au and, in the case of Al, Bi, and Au, for the same specimens in the solid phase. Peaks due to surface and volume plasmon excitation dominated the loss spectra for all elements except Au. The relative intensity of these peaks varied rapidly with scattering angle for the Al, Bi, In, and Ga specimens, but there was little angular variation when Al, Bi, or Au was evaporated onto a frozen substrate of the same element. The Al plasmon losses varied with temperature and changed at the melting point as would be expected from the known density variation. Changes in the Bi plasmon energy losses on melting and changes in other structure on melting have been interpreted in terms of band-structure changes. The peaks in the gold loss spectra appeared to become broader and less distinct on melting, from which it was concluded that the Au excited states had shorter lifetimes with increased disorder. In general, however, the liquid- and solid-state spectra of the same element were similar, thereby showing that for these materials there was not a large change in the electronic structure on melting.

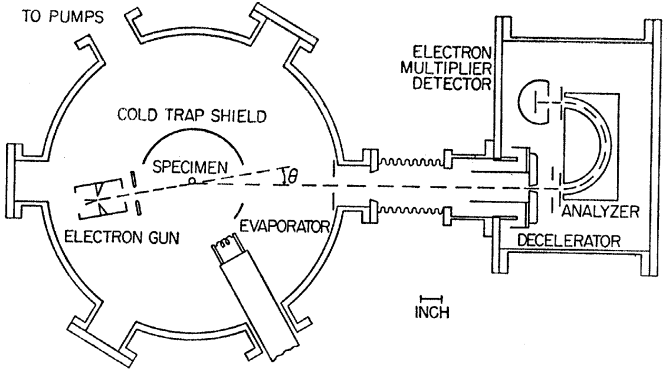

FIG. 1. Schematic outline of the apparatus.

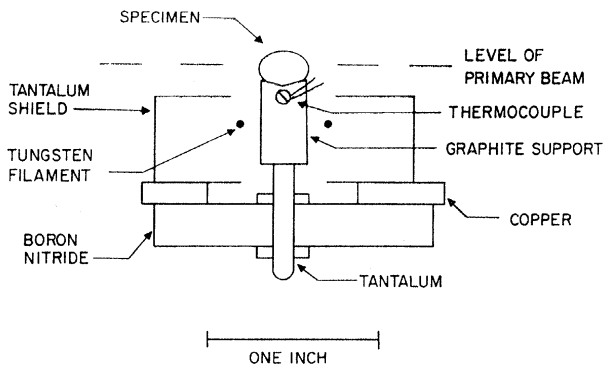

FIG. 2. Section through the specimen holder.

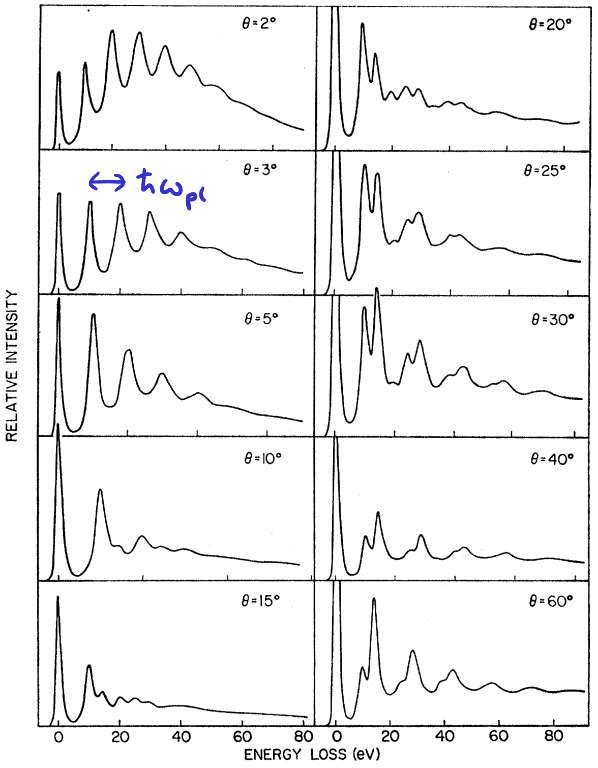

FIG. 3. Characteristic loss spectra of liquid Al for the total scattering angles θ indicated. These spectra have been traced from the original records and no direct comparison can be made between the different intensity scales; note also the different energy loss scales.

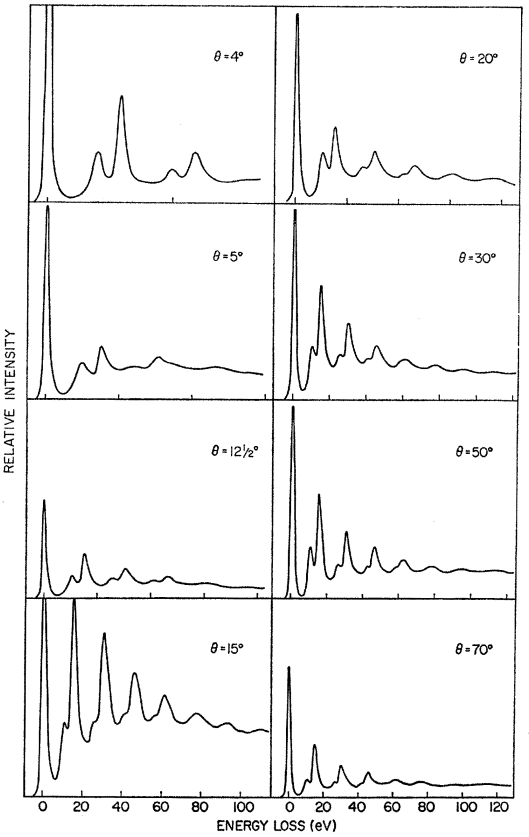

FIG. 5. Characteristic loss spectra recorded when Al was evaporated onto a frozen Al substrate for the scattering angles indicated. Note the different energy-loss scales.

• plasmon dispersion and e-h continuum via EELS

PHYSICAL REVIEW B VOLUME 40, NUMBER 15 15 NOVEMBER 1989-II

Valence-electron excitations in the alkali metals

A. vom Felde,* J. Sprösser-Prou, and J. Fink
Kernforschungszentrum Karlsruhe, Institut für Nukleare Festkörperphysik, P.O. Box 3640, D-7500 Karlsruhe, Federal Republic of Germany
(Received 13 March 1989)

To study the dynamical response of the valence-electron gas in nearly-free-electron metals, we carried out an electron-energy-loss investigation on Na, K, Rb, and Cs. On polycrystalline samples we measured the volume plasmon dispersion, which showed strong deviations not only from the random-phase approximation, but deviations as well from the predictions of the current theories for Fermi liquids, including short-range exchange and correlation. In addition, anomalous dispersion Both results may be traced back to exchange and correlation rent Fermi-liquid theories. Furthermore, we observed the ex- a and Rb, the dispersion of which yields the effective band s for Na are at variance with recently published enhancement ates. To elucidate the influence of band structure, measure- gle-crystalline Na film and we observed the so-called zone-

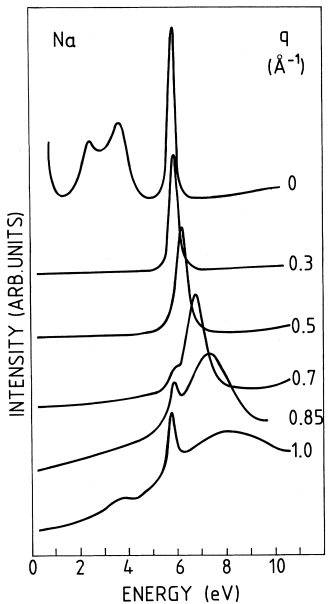

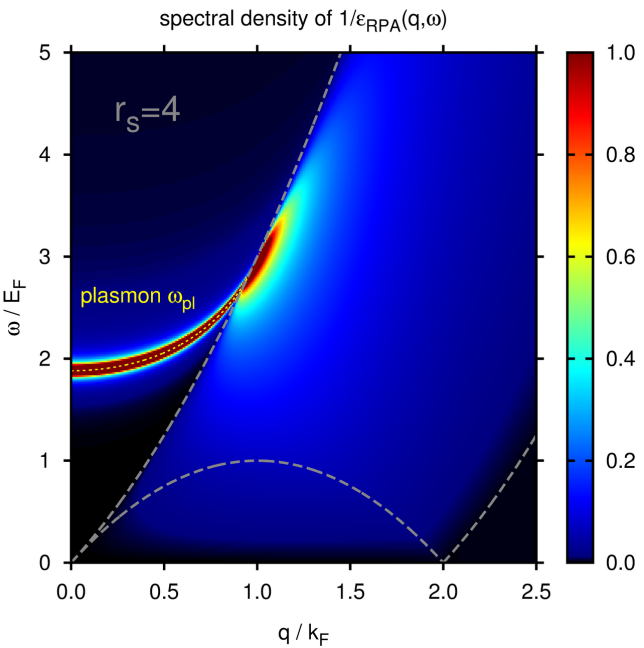

sodium

mass density $0.968\ g\,cm^{-3}$

molar density $22.99\ g\,mol^{-1}$

→ $r_s = 4.0$

$k_F = 0.91\ Å^{-1}$

$E_F = 3.1\ eV$

FIG. 1. Experimental energy-loss spectra of Na for different momentum transfers, demonstrating surface plasmons, the volume plasmon dispersion, and the onset of double scattering contribution at high q ($q > 0.7\ Å^{-1}$).

- shift of the plasmon energy and dispersion under high pressure by IXS

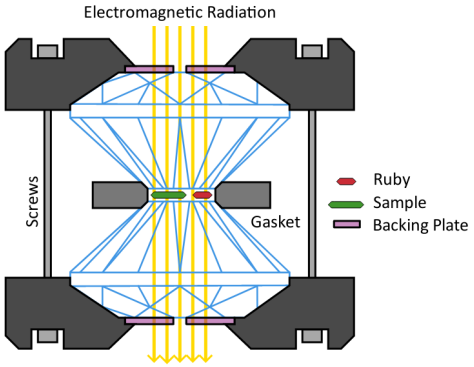

PRL **107,** 086402 (2011) PHYSICAL REVIEW LETTERS week ending 19 AUGUST 2011

Plasmons in Sodium under Pressure: Increasing Departure from Nearly Free-Electron Behavior

I. Loa,[1,*] K. Syassen,[1] G. Monaco,[2] G. Vankó,[2,†] M. Krisch,[2] and M. Hanfland[2]

[1]*Max-Planck-Institut für Festkörperforschung, Heisenbergstrasse 1, 70569 Stuttgart, Germany*
[2]*European Synchrotron Radiation Facility, BP 220, 38043 Grenoble Cedex, France*

(Received 21 December 2010; published 16 August 2011)

We have measured plasmon energies in Na under high pressure up to 43 GPa using inelastic x-ray scattering (IXS). The momentum-resolved results show clear deviations, growing with increasing pressure, from the predictions for a nearly free-electron metal. Plasmon energy calculations based on first-principles electronic band structures and a quasiclassical plasmon model allow us to identify a pressure-induced increase in the electron-ion interaction and associated changes in the electronic band structure as the origin of these deviations, rather than effects of exchange and correlation. Additional IXS results obtained for K and Rb are addressed briefly.

DOI: 10.1103/PhysRevLett.107.086402 PACS numbers: 71.45.Gm, 62.50.−p, 71.20.−b, 78.70.Ck

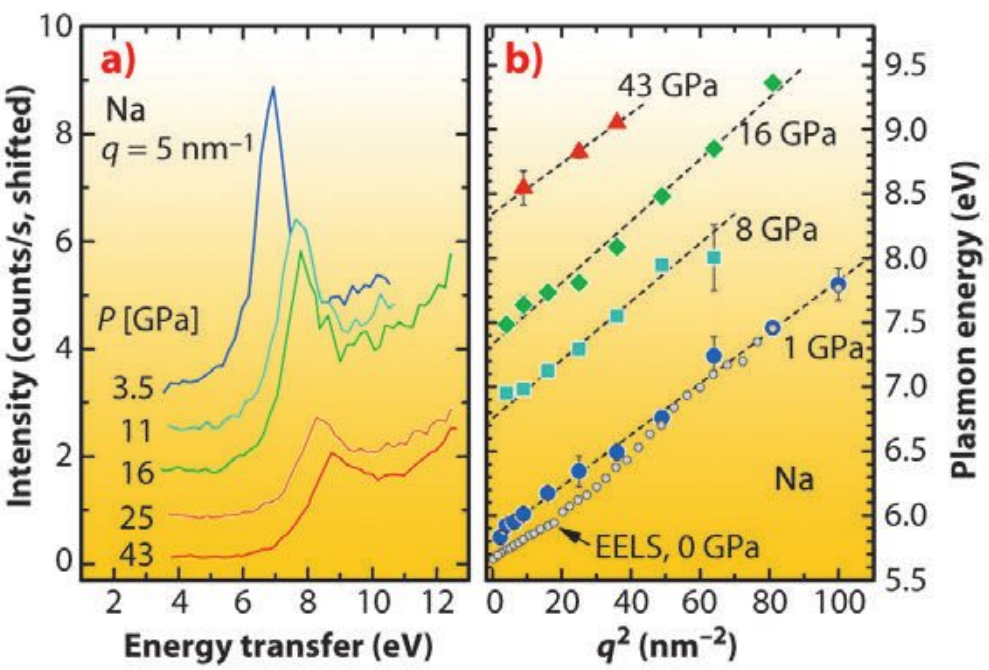

FIG. 1. IXS spectra of polycrystalline sodium pressurized in a diamond anvil cell. (a) Energy transfer spectra for a momentum transfer of $q = 5$ nm^{-1} and pressures of 3.5–43 GPa. (b) Energy transfer spectra of Na at 16 GPa and momentum transfers of 2–9 nm^{-1}. Vertical offsets are added for clarity.

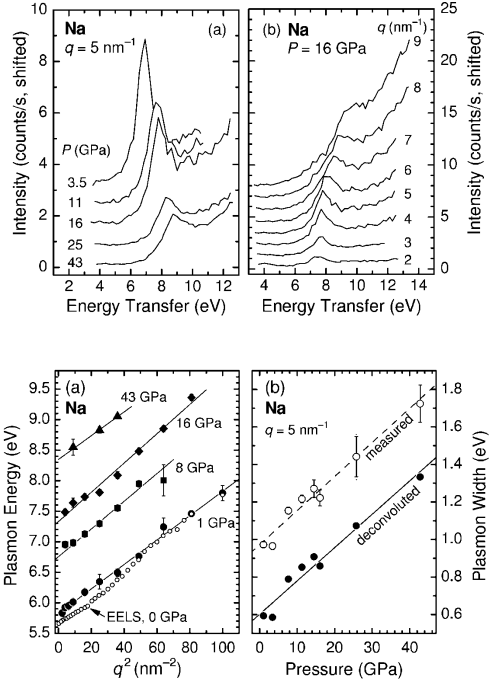

FIG. 3. (a) Plasmon dispersions $E(q^2)$ of polycrystalline Na as a function of pressure. Ambient-pressure electron-energy-loss spectroscopy results by vom Felde *et al.* [10] are indicated by small open symbols. (b) Plasmon linewidth of Na versus pressure.

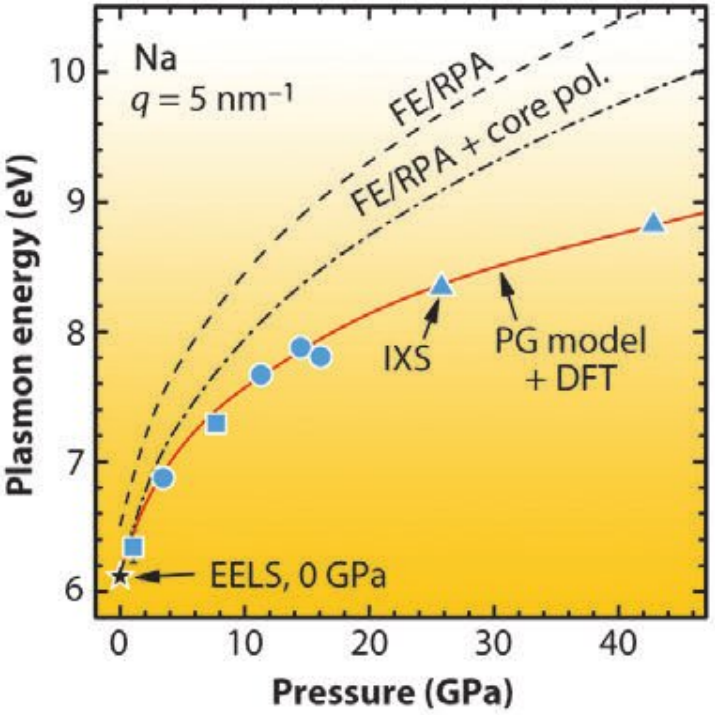

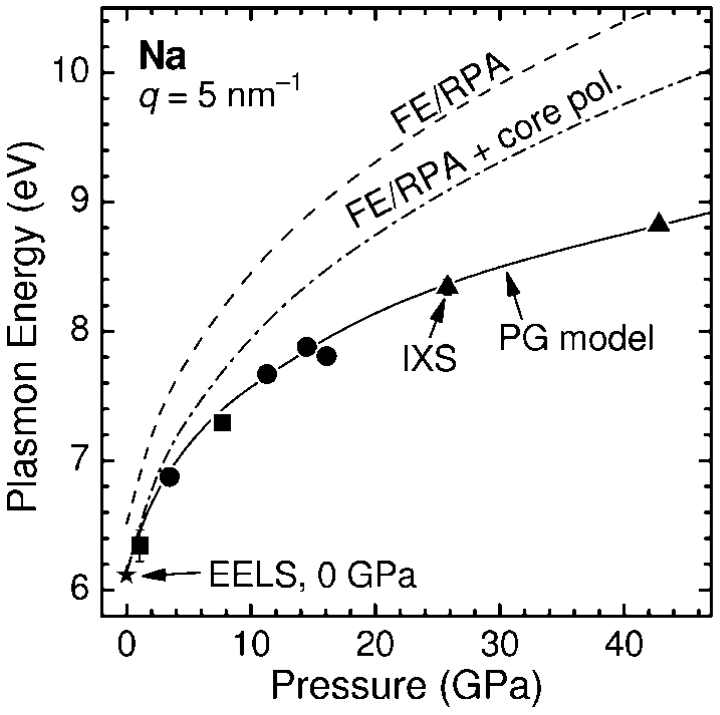

FIG. 4. Experimental pressure dependence of the directionally averaged plasmon energy in Na at $q = 5$ nm^{-1} (large symbols) and results of the free-electron (FE) gas model, FE model with core polarization, and the PG model (solid line). The star indicates the ambient-pressure EELS result [10].

6 Electron renormalization within RPA

- selfenergy

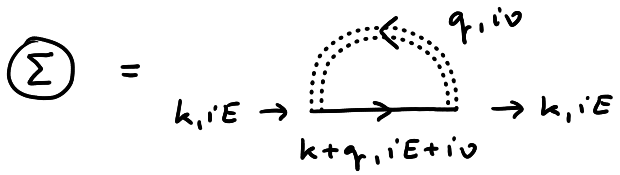

$$\Sigma(k,iE) = -\sum_q \frac{1}{\beta}\sum_{i\nu} \frac{V_q}{\varepsilon_{RPA}(q,i\nu)}\, G_0(k+q, iE+i\nu)$$

Hartree-Fock, plasmon & e-h continuum contribution

- renormalized retarded propagator

$$G_R(k,E) = \frac{1}{E - \varepsilon_k - \Sigma(k,E)}$$

poles of G_R correspond to quasielectron

→ solve $E - \varepsilon_k = \mathrm{Re}\,\Sigma(k,E)$

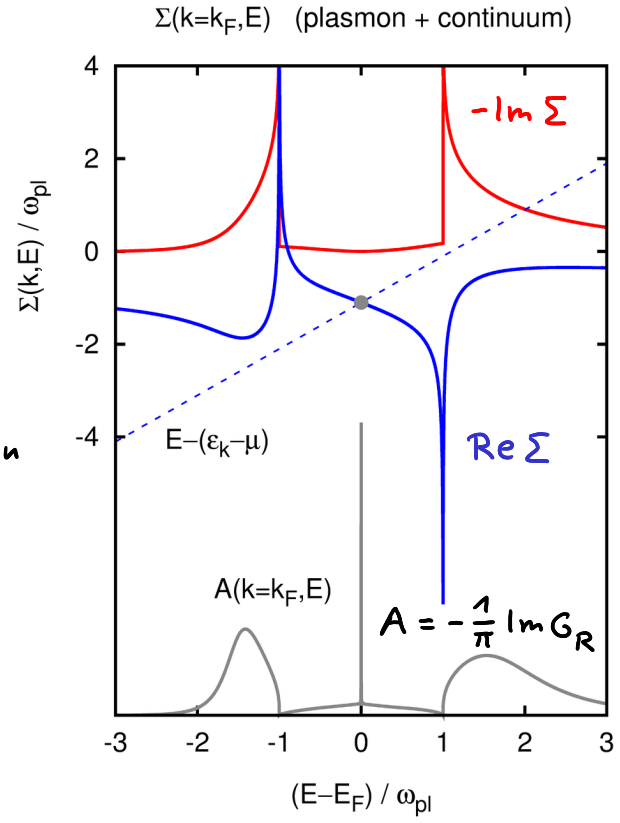

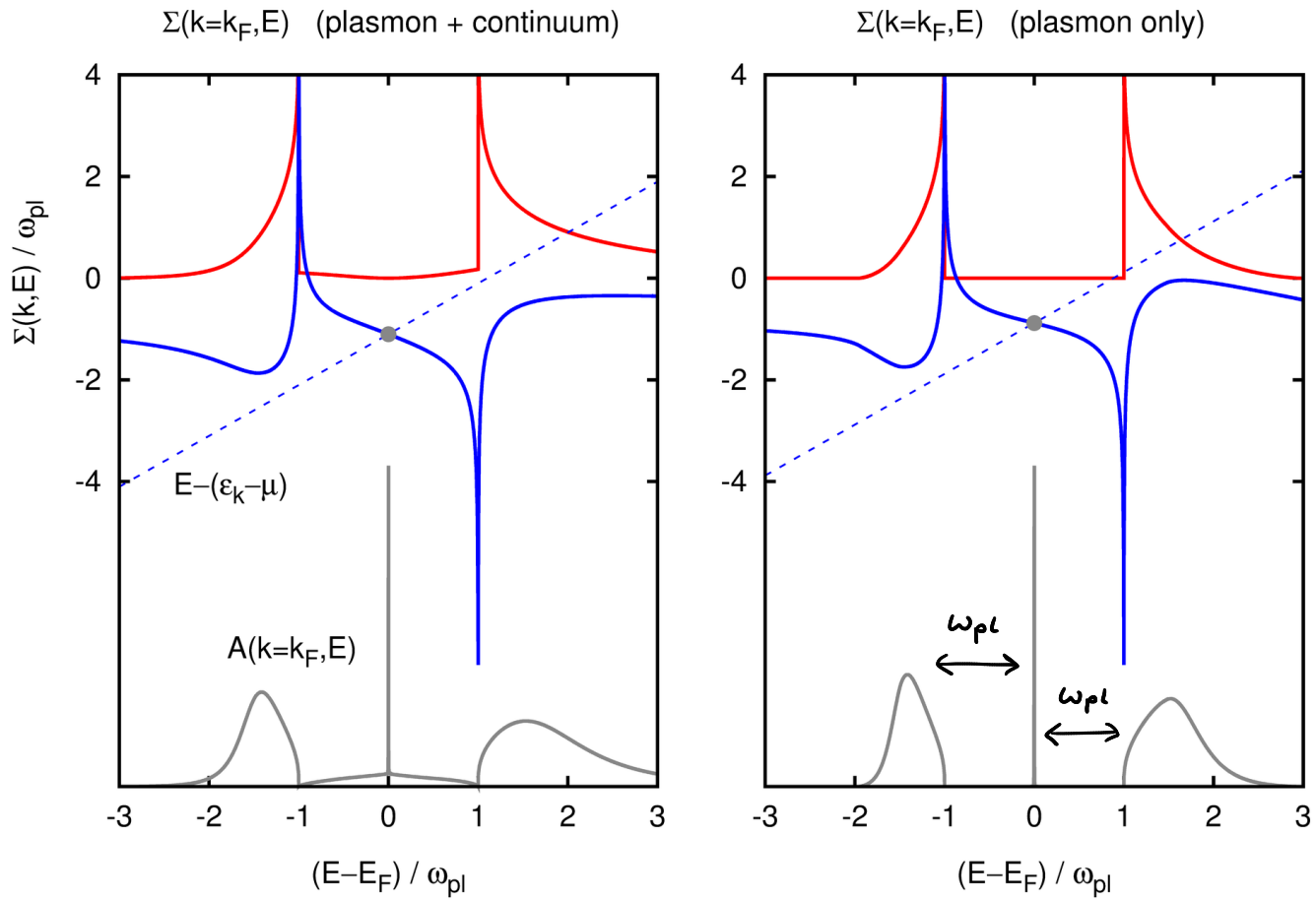
Σ(k=k_F,E) (plasmon + continuum)
Σ(k=k_F,E) (plasmon only)
Σ(k,E) / ω_pl
E−(ε_k−μ)
A(k=k_F,E)
ω_pl
ω_pl
(E−E_F) / ω_pl
(E−E_F) / ω_pl
4
2
0
-2
-4
-3
-2
-1
0
1
2
3

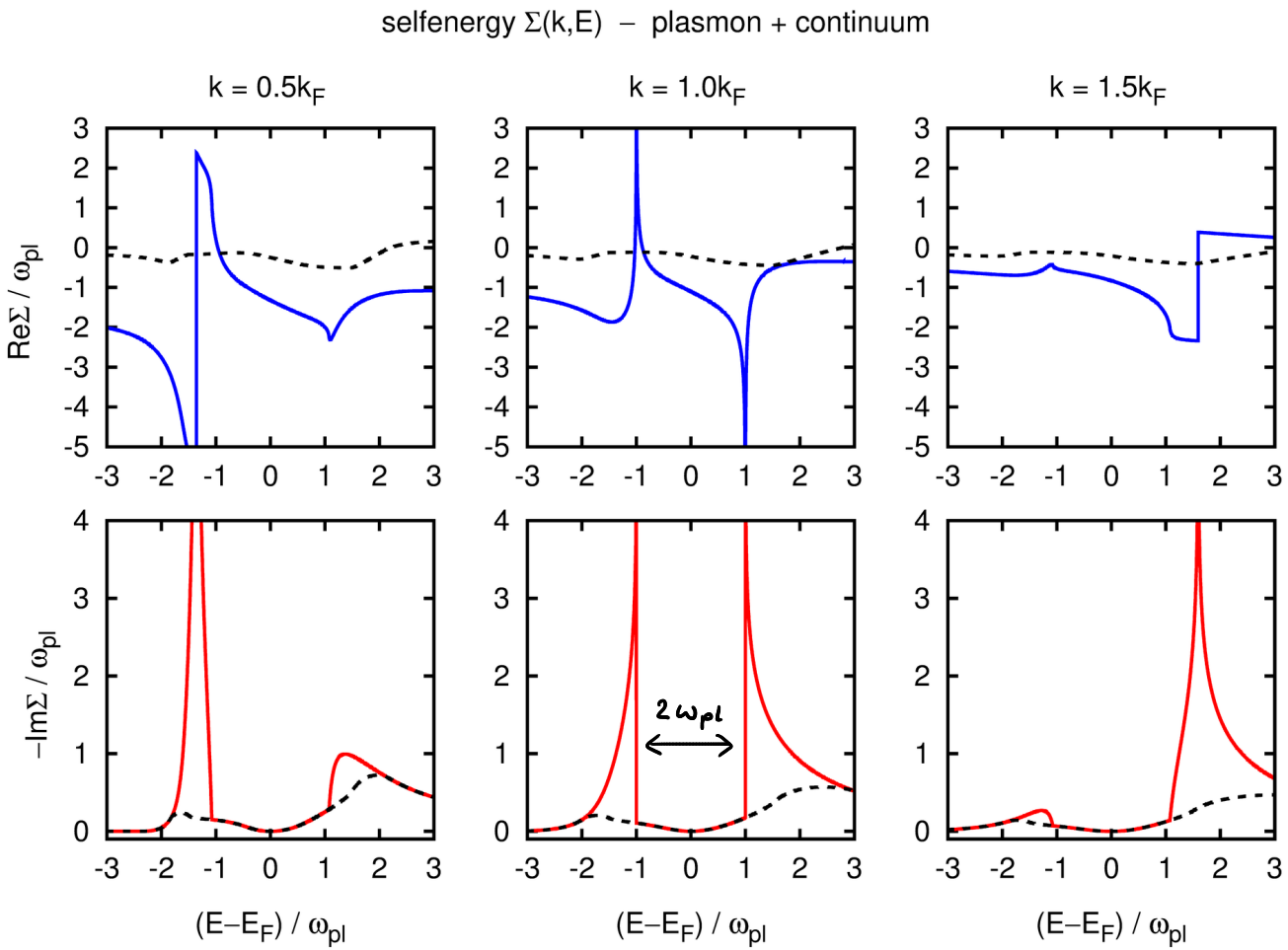
selfenergy Σ(k,E) – plasmon + continuum
k = 0.5k_F
k = 1.0k_F
k = 1.5k_F
ReΣ / ω_pl
−ImΣ / ω_pl
(E−E_F) / ω_pl
2 ω_pl

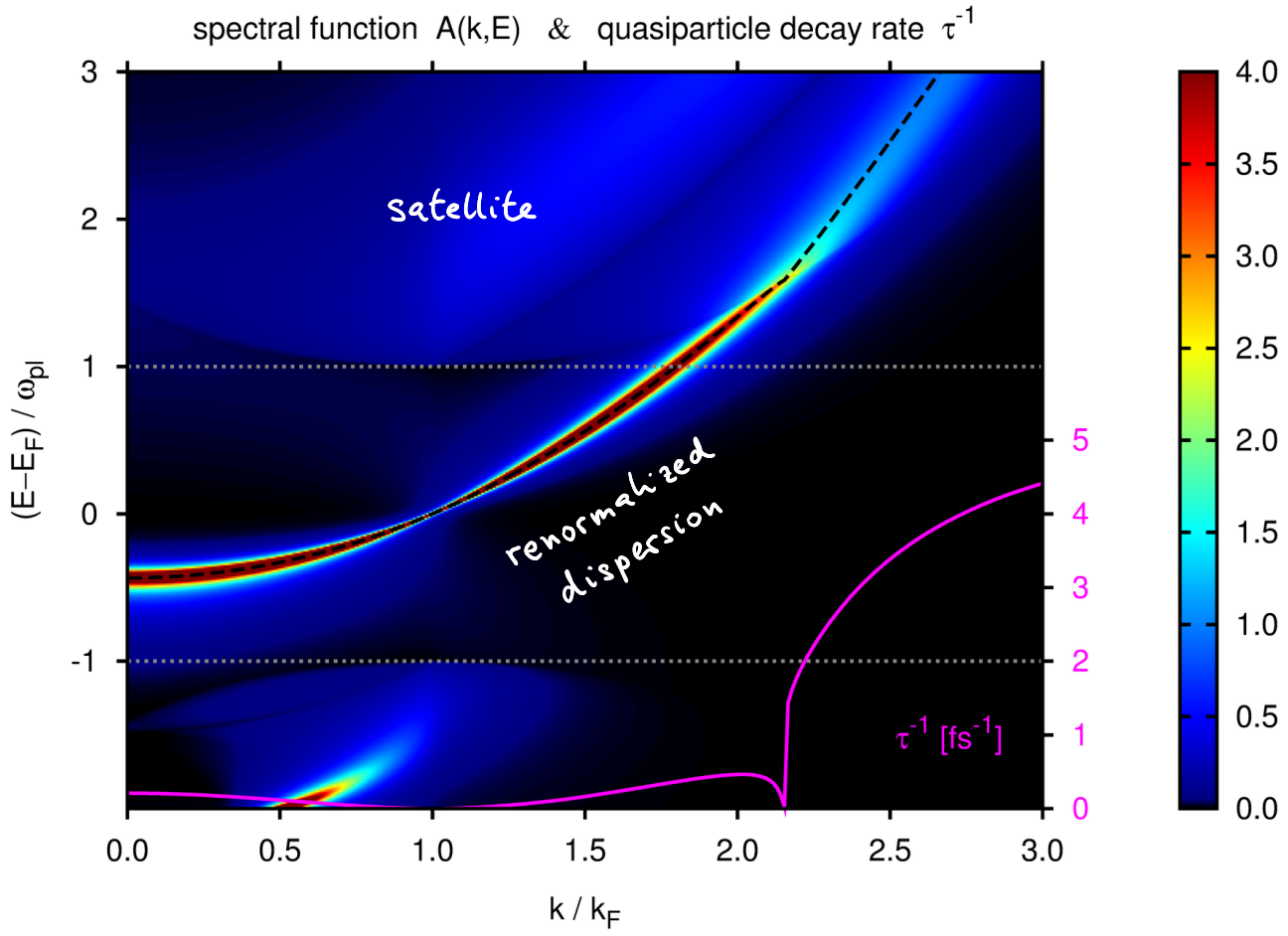
spectral function A(k,E) & quasiparticle decay rate τ^-1
satellite
renormalized dispersion
τ^-1 [fs^-1]
(E−E_F) / ω_pl
k / k_F
3
2
1
0
-1
0.0
0.5
1.0
1.5
2.0
2.5
3.0
5
4
3
2
1
0
4.0
3.5
3.0
2.5
2.0
1.5
1.0
0.5
0.0

- GW approximation and Swedish electron gas

selfenergy

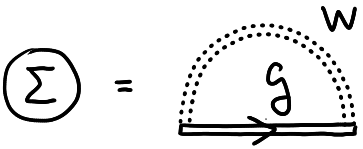

effective interaction (screened Coulomb)

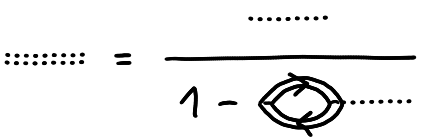

$$\Sigma = g * W \longleftarrow W(q,\omega) = \frac{V_q}{1 + V_q \Pi(q,\omega)}$$

selfconsistent scheme

$$g^{-1} = g_0^{-1} - \Sigma \longrightarrow \Pi = g * g$$

PHYSICAL REVIEW VOLUME 139, NUMBER 3A 2 AUGUST 1965

New Method for Calculating the One-Particle Green's Function with Application to the Electron-Gas Problem*

LARS HEDIN†
Argonne National Laboratory, Argonne, Illinois
(Received 8 October 1964; revised manuscript received 2 April 1965)

A set of successively more accurate self-consistent equations for the one-electron Green's function have been derived. They correspond to an expansion in a screened potential rather than the bare Coulomb potential. The first equation is adequate for many purposes. Each equation follows from the demand that a corre-

Phys. Rev. 139, A796 (1965)

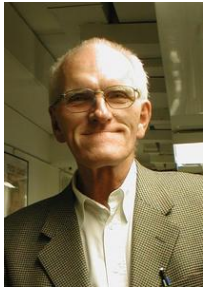

Lars Hedin (1930-2002)

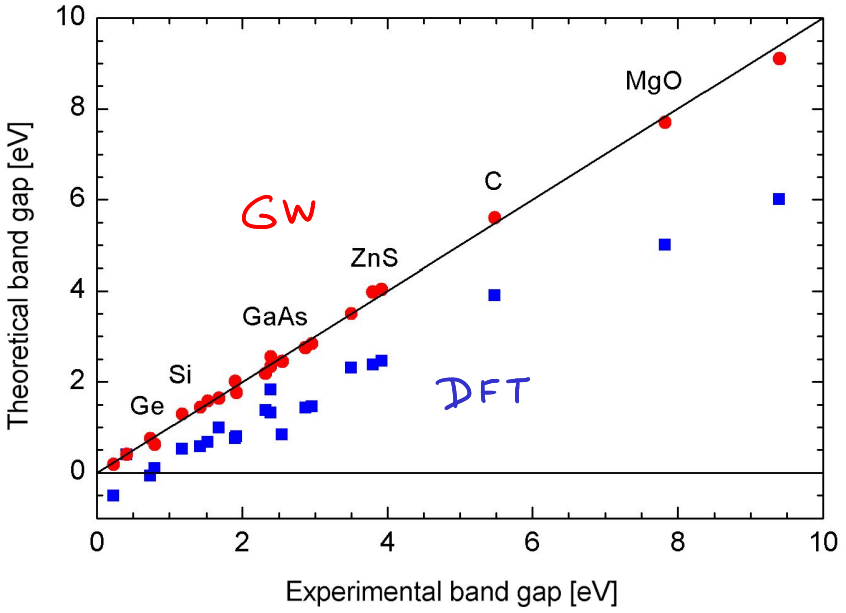

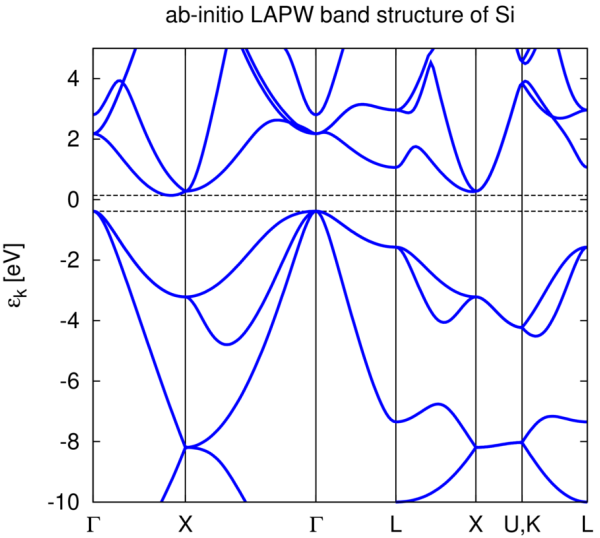

DFT is only a "ground state" theory, band structures are auxiliary

GW correctly captures dynamic screening & excitonic effects

- best ab-initio method for weakly correlated materials